

## A Nuclear Orientation Study of Terbium Ethyl Sulphate

*P. J. Back, B. Bleaney, G. J. Bowden<sup>A</sup> and N. J. Stone*

Mullard Cryomagnetic Laboratory, Clarendon Laboratory,  
Oxford University, Oxford OX1 3PU, U.K.

<sup>A</sup> On leave from School of Physics, University of New South Wales,  
N.S.W. 2052, Australia.

### *Abstract*

Terbium ethyl sulphate (TbES) has been studied by nuclear orientation using radioactive <sup>160</sup>Tb. It is found that (i) it is difficult to cool the terbium nuclei below  $\approx 50$  mK because of the long nuclear spin–lattice relaxation time  $T_{1N}$ ; (ii) application of small magnetic fields of the order 0.1 T produces a dramatic increase in the value of  $T_{1N}$ ; (iii) the long electronic relaxation time  $T_{1E}$  makes it difficult to determine the Curie temperature  $T_C$  in such experiments; and (iv) the saturation magnetic moment is approximately  $7.35 \mu_B$ . No nuclear magnetic resonance transitions were detected when radio-frequency fields at frequencies from 190 to 920 MHz were applied, but a long series of resonance absorption peaks was observed with a frequency separation of 26.3(3) MHz. Their origin is ascribed to magneto-acoustic modes within magnetic domains, rather than to magnetostatic modes, magnetic spin waves, or resonances within domain walls.

### 1. Introduction

Measurement of the hyperfine interactions for radioactive nuclei by means of magnetic resonance combined with nuclear orientation is a well established technique (NMR/ON). At a temperature of order 10 to 20 mK, with nuclear spin–lattice relaxation times ranging from 1 to  $10^3$  s, only low power is required to induce hyperfine transitions at frequencies of a few hundred MHz. For most nuclei of the lanthanide ions, however, the hyperfine interactions are large enough to produce considerable nuclear orientation at temperatures above 50 mK. Resonance then requires GHz frequencies, and relaxation times are of the order of milliseconds. Difficulties also arise because the wavelengths become shorter than the lengths of cable conveying power through the cryostat to the radioactive sample.

One case of NMR/ON for a lanthanide nucleus that has been reported is that of <sup>160</sup>Tb [ $I = 3$ , half-life 72 d, nuclear magnetic moment 1.658(8) nm] in ferromagnetic terbium metal. The magnetic interaction corresponds to a frequency of 1.385(1) GHz, but the large nuclear electric quadrupole interaction produces two transitions at much smaller frequencies for the three lowest hyperfine levels with the highest populations. These frequencies are 480.0(4) and 842.3(3) MHz respectively (Roman *et al.* 1986; Marshak *et al.* 1987). Even so, considerable difficulties were encountered due to inhomogeneous broadening of the transitions, and rapid thermal relaxation.

Below 221 K terbium metal is ferromagnetic, and the presence of conduction electrons gives relatively short relaxation times. However, inhomogeneous demagnetising fields produce linewidths of several MHz. By using ions implanted close to the centre of a small disc, where the fields are nearly uniform, Roman *et al.* (1986) reduced the linewidths to 2 MHz. However, this had the disadvantage that only 25 to 50% of the ions occupied normal lattice sites. Despite the decreased magnitude of the gamma-ray anisotropy, and nuclear relaxation times  $T_{1N}$  of some 5 ms at 25 mK, successful results were obtained.

Exploitation of non-metallic systems for orienting lanthanide nuclei has potential benefits for studies of both nuclear structure and the solid state. In this paper, experiments are described on an insulating crystal, where the absence of conduction electrons results in much longer relaxation times, which should make the search for resonance frequencies much easier than in a metal. Terbium ethyl sulphate,  $\text{Tb}(\text{C}_2\text{H}_5\text{SO}_4)_3 \cdot 9\text{H}_2\text{O}$  (TbES) was chosen; it has the advantage of a simple hexagonal crystal structure (Ketelaar 1937; Fitzwater and Rundle 1959). All the terbium ions are magnetically identical (point symmetry close to  $C_{3h}$ ), and their magnetic ground state has been determined in a magnetically diluted crystal by electron paramagnetic resonance (Baker and Bleaney 1958). Undiluted, TbES becomes ferromagnetic below 240 mK, with the moments ordered along the crystallographic  $c$ -axis (Hirvonen *et al.* 1975), as in the isostructural compound dysprosium ethyl sulphate (DyES). In the latter, the presence of long anti-parallel domains only about  $1 \mu\text{m}$  in width (Cooke *et al.* 1968*a*, 1968*b*) greatly reduces demagnetising effects. Given that TbES is similar to DyES, it is reasonable to expect relatively narrow NMR resonance lines in this compound. Finally, we note that proton NMR experiments have been successfully carried out in both DyES and TbES crystals in the mK region. In particular, the spatial coordinates of the protons have been determined using the NMR frequency shifts caused by the magnetic dipole fields of the  $\text{Dy}^{3+}$  and  $\text{Tb}^{3+}$  ions (see the review by Aminov and Teplov 1990).

Single crystals of TbES were grown from a saturated solution containing radioactive  $^{160}\text{Tb}$ , so all the nuclei occupied normal lattice sites. Experimental details are given in Section 3, but some difficulties soon became apparent. A long relaxation time prevents the nuclei being cooled below about 50 mK, at which the anisotropy of the 299 keV  $\gamma$ -ray from  $^{160}\text{Tb}$  is only about 8%. Also, application of a magnetic field of  $\approx 0.1$  T increases the relaxation time from minutes to several hours. A search over frequencies from 160 to 920 MHz revealed no genuine NMR transitions. Instead, a long series of resonance peaks was observed, separated by a frequency difference of  $26.3(3)$  MHz. These are ascribed to a pattern of 'standing waves', whose possible origins are discussed.

## 2. Theory

The crystal structure of TbES is hexagonal, and the electronic levels of the terbium ion  $\text{Tb}^{3+}$ ,  $4f^8$ ,  ${}^7F_6$ , split by the crystal field, have a doublet ground state, represented by the spin Hamiltonian (Baker and Bleaney 1958)

$$\mathcal{H} = DS_z + g_z \mu_B B_z S_z + AI_z S_z + P[I_z^2 - I(I+1)/3]. \quad (1)$$

The ground state doublet consists of two non-magnetic singlets, separated by

an energy  $D$  (Baker and Bleaney 1958; Hufner 1962), with wavefunctions

$$|a\rangle = 0.996|6^s\rangle + 0.10|0\rangle, \quad |b\rangle = |6^a\rangle, \quad (2)$$

where  $|6^s\rangle$ ,  $|6^a\rangle$  are the symmetric and antisymmetric combinations  $\sqrt{\frac{1}{2}}[|6\rangle \pm |-6\rangle]$ . All the other levels are some  $100 \text{ cm}^{-1}$  higher in energy and are not populated at low temperatures.

For the spin Hamiltonian (1), the energy levels are

$$W(m) = \pm \frac{1}{2}[D^2 + (g\mu_B B + Am)^2]^{1/2} + P[m^2 - I(I+1)/3], \quad (3)$$

where  $m$  is the nuclear magnetic quantum number. Diluted in YES, the paramagnetic impurities have  $g = 17.72$  and  $D = 0.387 \text{ cm}^{-1} = 11.6 \text{ GHz}$  (Baker and Bleaney 1958). These values should be substantially correct for undiluted TbES, where the value of  $D$  is estimated to be  $0.39 \text{ cm}^{-1}$  (Neogy *et al.* 1978). This estimate is in close agreement with that for the dilute compound, and hence  $D = 0.387 \text{ cm}^{-1}$  ( $11.6 \text{ GHz}$ ) is used in the following analysis.

For the single stable isotope  $^{159}\text{Tb}$  ( $I = \frac{3}{2}$ ) the magnetic hyperfine parameter is  $A/\hbar = +0.209 \text{ cm}^{-1} = +6.27 \text{ GHz}$  (Baker and Bleaney 1958). The value of the quadrupole splitting was not determined, but  $P/\hbar = 0.386 \text{ GHz}$  for the  $|J_z = \pm\rangle$  and  $+0.337 \text{ GHz}$  in terbium metal (Bleaney 1988, Tables 13, 14). An independent estimate based on the measurements of Easley *et al.* (1968) for  $^{160}\text{Tb}$ , together with average values of  $1.4(2) \text{ b}$  and  $3.0(6) \text{ b}$  ( $1 \text{ b} \equiv 10^{-28} \text{ m}^2$ ) for the quadrupole moments of  $^{159}\text{Tb}$  and  $^{160}\text{Tb}$ , gives  $^{159}P/\hbar = 0.38(3) \text{ GHz}$ . With this value, the energy levels at  $B = 0$  consist of four doublets, at  $\pm 7.467 + P/\hbar$  and  $\pm 6.008 - P/\hbar$  (GHz). In mK, they lie at 717, 610, 33 ( $\pm 1 \text{ mK}$ ) above the ground state.

When a field is applied, each electronic level with a given value of  $m$  produces a magnetic moment

$$M_z/g\mu_B = \pm (g\mu_B B + Am)/[D^2 + (g\mu_B B + Am)^2]^{1/2}, \quad (4)$$

where the alternative signs apply to the two electronic levels. To find the net moment at any temperature, (4) must be summed over all the  $m$  substates, weighted by appropriate Boltzmann factors. A plot of the calculated magnetic moment versus applied magnetic field can be seen in Fig. 1 for a temperature of  $50 \text{ mK}$ .

In considering the ordered structure, a natural starting point is provided by the measurements of Cooke *et al.* (1968a) on the isostructural compound DyES. The magnetic moment of each dysprosium ion is  $g/2 = 10.8/2 = 5.4 \mu_B$ . Further, dipolar interactions between the ions produce ferromagnetic chains along the  $c$ -axis of the crystal, with a Curie temperature  $T_C = 130 \text{ mK}$ . Similar effects are expected in TbES, for which a preliminary estimate of  $T_C$ , obtained from the ratio of the values of the  $(g/2)^2$  along the  $c$ -axis, is  $130 \times (8.86/5.4)^2 = 360 \text{ mK}$  for TbES. However, the splitting term  $D$  in equation (5) reduces the magnetic moment  $\langle M \rangle$  from  $8.86$  to  $8.45 \mu_B$  for small fields at low temperatures. Thus the expected value of  $T_C$  should be correspondingly smaller, about  $320 \text{ mK}$  (almost independent of the hyperfine interactions), closer to the measured value of  $240 \text{ mK}$  (Hiroven *et al.* 1975).

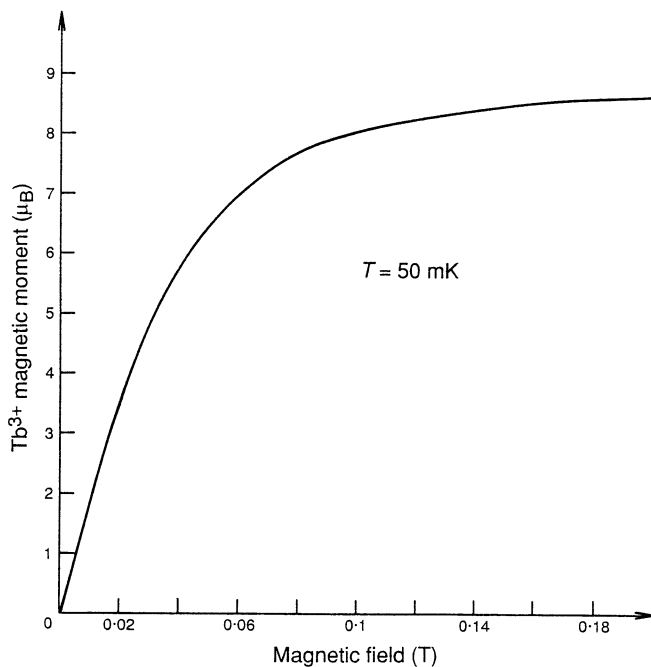


**Fig. 1.** Calculated magnetic moment as a function of magnetic field at 50 mK; for 100 mK the curve is almost identical.

In DyES, the internal magnetic field at each ion in a ferromagnetic chain is 0.0713 T (Cooke *et al.* 1968*a*). Scaled up in the ratio of the moments ( $8.45/5.4$ ), this becomes 0.112 T for TbES. In this field, the energy levels are spread over nearly 1900 mK, and practically all the  $^{159}\text{Tb}$  nuclei are in the lowest hyperfine level. The energy levels for an internal field of 0.112 T are listed in Table 1.

For  $^{159}\text{Tb}$  nuclear transitions should occur at frequencies of between 2.06 and 4.14 GHz, well above those for  $^{160}\text{Tb}$ ,  $I = 3$ , shown in Table 2, from Easley *et al.* (1968). These frequencies are assumed to be solely determined by the host ions  $^{159}\text{Tb}$ . However, excitation of a nuclear transition  $|m = 3\rangle$  to  $|m = 2\rangle$  for  $^{160}\text{Tb}$  causes a small reduction in the electronic moment of the parent ion, and a frequency shift of order 0.07 GHz.

In a typical experiment, not all of the  $^{159}\text{Tb}$  nuclei are in the lowest level, and the electronic moments vary slightly, producing some line broadening of the NMR transitions. Their strength depends also on the NMR enhancement factor  $\kappa$ , in the plane normal to the  $c$ -axis, for which an estimate from Larsen and Jeffries (1966) gives a rather small value of  $\kappa \approx 2$ . Thus searches for the NMR/ON resonance frequencies of the radioactive nuclei need the highest rf power consistent with keeping the heating of the crystal to a minimum.

### 3. Experimental Details

Single crystals of TbES containing radioactive  $^{160}\text{Tb}$  were grown from a saturated solution at  $\approx 20^\circ\text{C}$  under a pressure of  $\approx 10$  cm Hg ( $\equiv 13.3$  kPa). Single crystals, each with an activity of about  $2 \mu\text{Ci}$  ( $1 \mu\text{Ci} \equiv 3.7 \times 10^4$  Bq) and

**Table 1. Energy levels of the TbES from equation (5)**

Here  $g = 17.72$ ,  $D = 0.387 \text{ cm}^{-1} = 11.6 \text{ GHz}$ , and  $B = 0.112 \text{ T}$ . The left-hand side is for the isotope  $^{159}\text{Tb}$ ,  $I = \frac{3}{2}$ ,  $A/\hbar = +6.27 \text{ GHz}$ ,  $P/\hbar = 0.38 \text{ GHz}$ . The right-hand side is for the isotope  $^{160}\text{Tb}$ ,  $I = 3$ ,  $A/\hbar = 2.648(24) \text{ GHz}$ , and  $P/\hbar = +0.165(15) \text{ GHz}$

$^{159}\text{Tb}$				$^{160}\text{Tb}$			
Levels		Splitting	Energy	Levels		Splitting	Energy
$S_z$	$I_z$	(GHz)	(mK)	$S_z$	$I_z$	(GHz)	(mK)
+1/2	+3/2	+19.85	1869	+1/2	+3	+19.60	1802
+1/2	+1/2	+16.13	1689	+1/2	+2	+17.52	1702
+1/2	-1/2	+13.24	1551	-1/2	+1	+15.78	1619
+1/2	-3/2	+11.24	1455	+1/2	0	+14.39	1552
				+1/2	-1	+13.34	1502
-1/2	-3/2	-10.48	413	+1/2	-2	+12.64	1468
-1/2	-1/2	-14.00	244	+1/2	-3	+12.31	1452
-1/2	+1/2	-16.88	106				
-1/2	+3/2	-19.09	0	-1/2	-3	-10.66	349.9
				-1/2	-2	-12.64	254.8
				-1/2	-1	-14.33	173.7
				-1/2	0	-15.71	107.5
				-1/2	+1	-16.77	56.5
				-1/2	+2	-17.52	20.6
				-1/2	+3	-17.95	0

**Table 2. Predicted frequencies for the NMR transitions between the sublevels of  $^{160}\text{Tb}$  ( $I = 3$ ) in the lower electronic level of TbES, in a field of 0.112 T**

The hyperfine parameters are  $A/\hbar = 2.648(24) \text{ GHz}$ ,  $P/\hbar = +0.165(15) \text{ GHz}$

Transition	-3 ↔ -2	-2 ↔ -1	-1 ↔ 0	0 ↔ +1	+1 ↔ +2	+2 ↔ +3
Frequency (GHz)	0.430(76)	0.749(46)	1.065(19)	1.381(19)	1.685(46)	1.985(76)

well defined faces, some 3 mm in the longest dimension, were selected for the experiments. The  $c$ -axis was identified using a polarising microscope.

An Oxford Instruments DR400 dilution refrigerator with a thin, flat copper cold finger (dimensions  $5 \times 10 \times 1 \text{ mm}$ ) was used to obtain temperatures in the mK regime. These could be set anywhere between 10 and 300 mK. A single crystal of TbES was glued with colloidal silver paint to one side of the finger. The  $c$ -axis of the crystal was vertical, and normal to the axis of a simple Helmholtz coil providing the radio-frequency field. The orientation was such that eddy-current heating in the copper finger was reduced to a minimum. For temperature measurements below 30 mK, a  $\approx 0.2 \mu\text{Ci } ^{60}\text{Co/Fe}$  nuclear orientation thermometer was soft-soldered to the other side of the copper finger. This consisted of a thin polycrystalline disk of iron about 4 mm in diameter and about 100  $\mu\text{m}$  thick. For reliable temperature measurements, a small polarising field of  $\approx 0.1 \text{ T}$  is required. However, such a field is sufficient to drive out the domain walls and magnetically saturate the TbES crystal. Consequently, a field of 0.04 T was used, since this is too small to penetrate inside the ferromagnetic domains in TbES and so does not disturb the internal field of 0.112 T (Aminov and Teplov 1990). However, it should be acknowledged that a field of only 0.04 T is not sufficient to fully

polarise the Fe magnetic moments, so the  $^{60}\text{Co}/\text{Fe}$   $\gamma$ -ray anisotropy measurements, shown below in Fig. 4, can only be used as a qualitative (overestimate) guide to the temperature of the copper finger. Higher temperatures were determined by means of a calibrated Speer resistance thermometer.

Finally, the  $\gamma$ -ray counts for both the  $^{60}\text{Co}$  and  $^{160}\text{Tb}$  isotopes were acquired using a GeLi detector in the PHA mode. This allowed any movement of the peaks during the course of the experiment to be tracked, and corrections applied. Background stripping of the  $\gamma$ -ray peaks in question was carried out using linear interpolation between the upper and lower window settings.

#### 4. Results and Nuclear Orientation

The angular distribution of the  $\gamma$ -rays was measured by two GeLi detectors, an ‘axial’ detector, 10 cm vertically below the crystal, and an ‘equatorial’ detector also 10 cm away, normal to the finger. The  $\gamma$ -ray anisotropy of the 299 keV gamma transition (pure E1,  $2^- \rightarrow 2^+$ ) was analysed with the usual formula

$$W(\theta) = 1 + B_2 U_2 A_2 P_2(\cos\theta), \quad (5)$$

where  $U_2 = 0.8281$ ,  $A_2 = -0.42(2)$  from Krane and Steffen (1970, 1971) and Fox *et al.* (1974);  $B_2$  is the thermal orientation parameter. As expected, the ratio of the anisotropies, equatorial to axial, was found to be  $-\frac{1}{2}$  within experimental error. Hot counts were taken with the TbES crystal at 1 K.

The measured axial anisotropy for the 299 keV  $\gamma$ -ray in zero magnetic field is shown as a function of temperature in Fig. 2. The same values are obtained with  $B = 0.04$  T. Data were collected for each point for a time of about 800 s. The figure shows that the largest anisotropy is only about 8%, much less than expected for a full electronic terbium moment. This indicates that the nuclei lose thermal contact with the cold finger, and  $T_{1N}$  becomes very long below about 50 mK. Nuclear relaxation processes are reduced by the small enhancement factor  $\kappa$ , normal to the  $c$ -axis (see Section 2).

It will be observed, from a comparison between the experimental and theoretical fits shown in Fig. 2, that it is difficult to fit the nuclear orientation results using the hyperfine frequencies in Table 2. However, if we assume that the  $\text{Tb}^{3+}$  magnetic moment is some 17% smaller than our theoretical estimate, a better fit to the NO data can be obtained. The electronic moment then becomes  $\approx 7.35 \mu_B$  and the predicted value of  $T_C$  is  $\approx 265$  mK, even closer to the measured value of 240 mK. However, it should be acknowledged that the use of a single magnetic moment is questionable, particularly when the temperature is close to  $T_C$ .

Finally, the rapid variation of the anisotropy in a slowly varying magnetic field  $B$  is shown in Fig. 3. It falls to less than 2%, but recovers quickly when the magnetic field is removed. This, combined with a large increase in  $T_{1N}$  (see Section 6), severely restricted the range of our experiments.

#### 5. Search for Magnetic Resonance

Power from a Marconi 1024 MHz frequency synthesizer, frequency modulated by  $\pm 0.5$  MHz, was used to search for magnetic resonance transitions. At intervals of 1 MHz, from 190 to 920 MHz,  $\gamma$ -ray counts were taken for 300 s using the

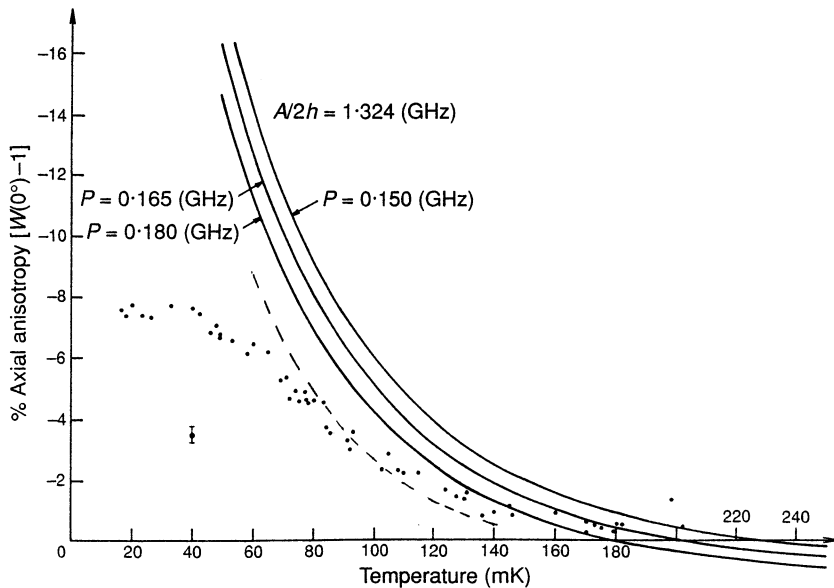


**Fig. 2.** Measured values of the axial anisotropy of the 299 keV  $\gamma$ -ray of  $^{160}\text{Tb}$  from 20 to 240 mK in zero applied field. The solid curves are calculated from Table 2. The dashed curve corresponds to a reduction in the electronic moment to  $7.35 \mu_B$ .

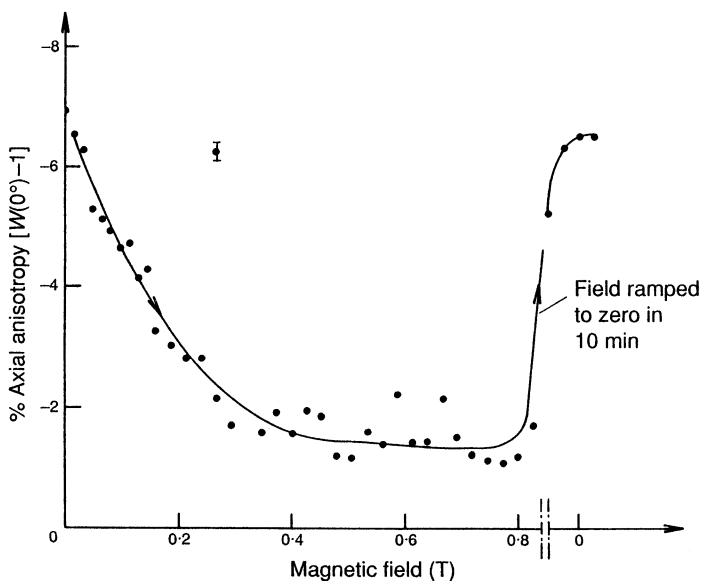


**Fig. 3.** Measured axial anisotropy of the 299 keV  $\gamma$ -ray of  $^{160}\text{Tb}$  in a magnetic field, increasing over two hours from 0 to 0.8 T.

largest rf power available (1 V into a nominal 50  $\Omega$ ). A series of peaks in the anisotropy between 300 and 620 MHz was observed; Fig. 4 shows that they are correlated with peaks in the readings of the  $^{60}\text{Co}/\text{Fe}$  thermometer. Their

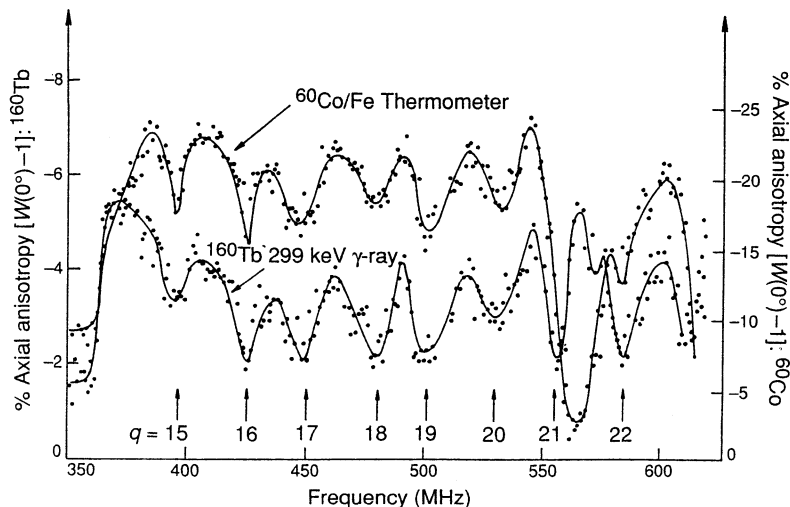


**Fig. 4.** Search for NMR/ON transitions of radioactive  $^{160}\text{Tb}$  from 350–620 MHz, in a field of 0.04 T. The figure shows the correlation between the  $^{160}\text{Tb}$  299 keV  $\gamma$ -ray axial anisotropy and the temperature (qualitative only) of the dilution refrigerator, as measured by a partially saturated  $^{60}\text{Co}/\text{Fe}$  thermometer. Strong rf coil resonances at  $\approx 350$  and 560 MHz were observed.

positions and intensities, independent of the depth of the frequency modulation, cannot be associated with nuclear transitions.

Reductions in the anisotropy at frequencies of 398, 425, 448, 480, 502 and 531 (all  $\pm 3$ ) MHz arise from heating of the crystal by the rf field. A reduction in the anisotropy to 2% corresponds to a temperature close to 125 mK, at which the  $T_{1N}$  is quite short. The heat must flow through to the copper finger, but without warming it by more than 20 mK. At 565 MHz, a sharp rise occurs in the temperature of the  $^{60}\text{Co}/\text{Fe}$  thermometer, but not in that of the TbES crystal. Since the smallest thermometer anisotropy corresponds to a cold finger temperature of  $\approx 60$  mK and the  $^{160}\text{Tb}$  nuclei never cool below  $\approx 70$  mK, this apparent difference in response is understandable if the heating is direct to the cold finger. The effect is taken to be an rf coil resonance which gives greatly increased eddy-current heating in the cold finger and thermometer. On either side of this, a series of peaks is recorded in the  $^{160}\text{Tb}$  anisotropy response, whose frequencies are plotted in Fig. 5 against an integer  $q$ , chosen to give a straight line passing through the origin. They are separated by 26.3(3) MHz; a missing peak at 368 MHz ( $q = 14$ ) is ascribed to resonance in the rf coil. The absence of peaks at  $q = 28, 29$  is more difficult to explain, but the results suggest the presence of ‘standing waves’ in the TbES crystal (see Section 7 below).

At first sight, it was believed that the ‘peaks’ shown in Fig. 4 must be due to standing waves in the rf cable. To check this hypothesis, measurements were made using a simple BNC T-junction placed at the output of the Marconi generator to monitor reflections. Standing waves were indeed observed, from 350 MHz to 620 MHz, but at a frequency separation of 8.65 MHz. This result was used, in conjunction with a cable velocity of  $2 \times 10^8 \text{ ms}^{-1}$ , to determine the length of the rf cable. The calculated length was found to be 11.5(1) m, in excellent agreement with direct measurement.

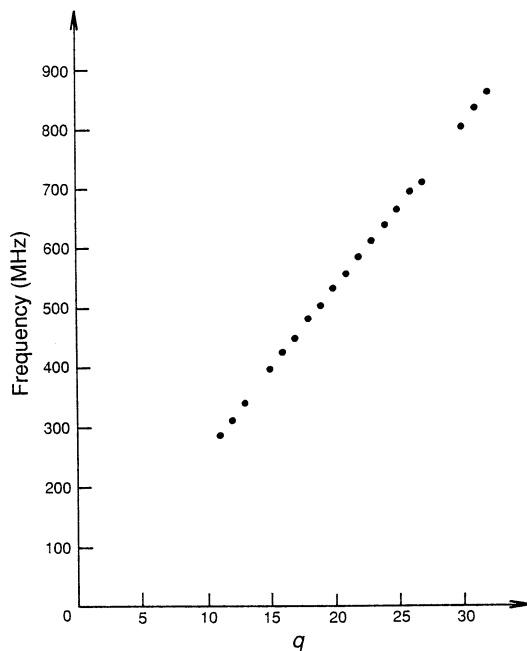


Fig. 5. Standing-wave resonances plotted against the integer  $q$ , chosen to make the straight line pass through zero at  $q = 0$ .

However, it should be acknowledged that the rf cable from the Marconi frequency source to the NMR/ON coil consisted of at least two sections, both nominally  $50 \Omega$ , but of dissimilar lengths. Thus the possibility of standing waves in smaller sections of the rf cable could not be ruled out *a priori*. Consequently, a run with a fully polarised  $^{60}\text{Co}/\text{Fe}$  thermometer, but without the TbES crystal, was performed to see if standing waves in the rf cable could give rise to the peaks witnessed in the  $^{60}\text{Co}/\text{Fe}$  record shown in Fig. 4. A strong rf coil resonance at  $\approx 350$  MHz was observed through a temperature rise in the copper finger from 10 to 30 mK, but no such increases, in excess of 2 mK, were observed in the frequency range near  $q = 15$  to 19, where the TbES crystal is at  $\approx 125$  mK. Thus the peaks witnessed in TbES cannot be ascribed to standing waves in the rf cable.

In another experiment, with the TbES crystal in place, a traverse from 450 to 611 MHz was made, but this time in zero applied field. The  $^{160}\text{Tb}$  peaks at  $q = 17$  to 23 shown in Fig. 5 were observed, indicating that the weak polarising field of 0.04 T used for the  $^{60}\text{Co}/\text{Fe}$  thermometer in the first set of experiments has little effect.

## 6. Nuclear Relaxation in Applied Fields

Maximum rf power was applied at 502 MHz ( $q = 19$ ), in various applied magnetic fields. After the NO signal had reached saturation, the rf field was reduced to zero; the recovery of the NO signal (see Fig. 6) shows that in a field of 0.061 T, the nuclear spins cool to about 50 mK in 30 min ( $1.8 \times 10^3$  s).

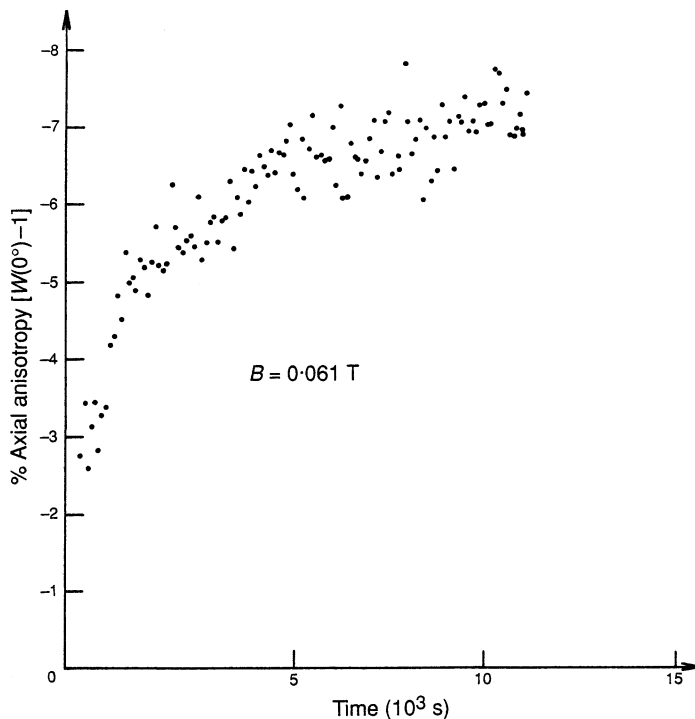


**Fig. 6.** Axial anisotropy of the 299 KeV  $\gamma$ -ray of  $^{160}\text{Tb}$  as a function of time in a field of 0.061 T, after the removal of the radio-frequency excitation.

In fields above 0.1 T the value of  $T_{1N}$  increases rapidly to many hours, but fields less than 0.06 T have little effect on  $T_{1N}$ . We interpret these results as follows. In small fields, domain walls are present in the crystal. Cooke *et al.* (1968*a*, 1968*b*) have argued that within a domain wall, which is very thin, the dipolar field is about 35% smaller than that of a domain. Consequently, thermal fluctuations of the Tb electronic moments (along the *c*-axis) will be larger in domain walls, giving rise to enhanced nuclear relaxation over a considerable range. Thus while the domain walls remain in the crystal, the relaxation mechanism is approximately independent of the applied field. However, in higher fields this mechanism is lost to the system: the domain walls are removed and the Tb electronic moments approach magnetic saturation. In this regime therefore, very long relaxation times are to be expected.

## 7. Standing Waves in the Crystal

The results suggest that rf power is absorbed through the presence of standing waves in the crystal of TbES. One possible source of the standing waves would be magneto-static modes (Walker 1957, 1968; Storey *et al.* 1977). In thin films, resonance occurs when the thickness is an integral number of half-wavelengths, but spin waves have also been observed in bulk material. However, in neither

case do the frequencies vary linearly, unlike those shown in Fig. 5. Here the linear progression of frequencies resembles that for magneto-acoustic waves, as observed in thin films of the ferromagnetic yttrium iron garnet (Dötsch 1978; Dötsch *et al.* 1978). The wave velocity deduced was close to that of sound. The formula

$$f = (c/2t)q, \quad (6)$$

where  $f$  is the frequency and  $t$  the thickness, was applied to TbES, and taking  $t = 1.5 \text{ mm}$ , the distance between the two flat faces, leads to a velocity  $c$  of  $\approx 7.9 \times 10^4 \text{ m s}^{-1}$ . This is well above measured speeds in similar materials. On the other hand, if  $t$  is taken to be  $\approx 1 \mu\text{m}$ , the width of a domain, the velocity is much too small. A possible explanation is that the domains take the form of strips, only  $\approx 1 \mu\text{m}$  wide, but appreciably longer. For a plausible velocity of  $3.5 \times 10^3 \text{ m s}^{-1}$ , a length of  $33 \mu\text{m}$  is needed. The magnetic energy of such strip domains is comparable with that of the needle domains postulated by Cooke *et al.* (1968*b*). Two possible domain structures are shown in Fig. 7. To give minimum energy, the domain walls should follow the symmetry of the hexagonal lattice.

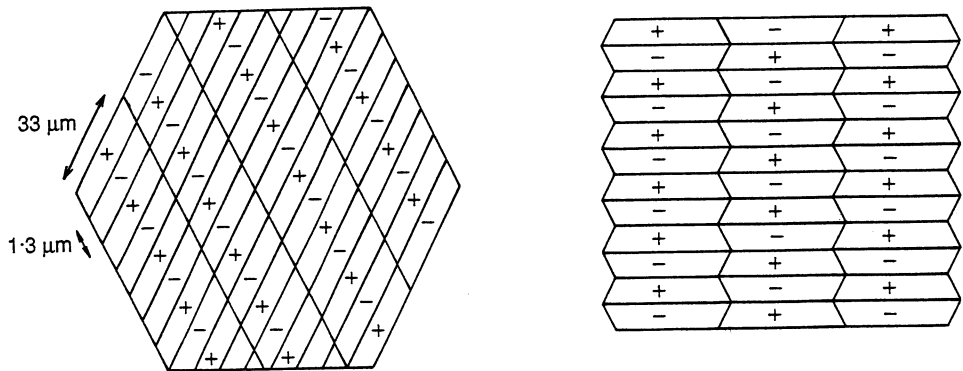


Fig. 7. Possible domain structures in TbES, with hexagonal symmetry.

## 8. Conclusion

Single crystals of TbES containing radioactive  $^{160}\text{Tb}$  have been studied using nuclear orientation techniques. The results show that the length of the nuclear spin lattice time  $T_{1N}$  makes it difficult to cool the nuclei below about 50 mK, and that  $T_{1N}$  increases very rapidly when magnetic fields above about 0.1 T are applied. At low temperatures, the electronic magnetic moment is  $\approx 7.35 \mu_B$  and the application of radio-frequency fields between 190 and 920 MHz induces a series of absorption maxima at frequencies with a constant separation of 26.3 MHz. These are ascribed to magneto-acoustic standing waves that cause irreversible heating of the crystal and diminution of the  $\gamma$ -ray anisotropy. Plausible velocities of sound are obtained for domains of dimensions  $1 \times 33 \mu\text{m}$ .

To verify this hypothesis, direct examination of the domain structure would be required. Faraday rotation has been used to observe oscillations in stripe domains in YIG by MacNeal and Humphrey (1979), and Argyle *et al.* (1983), but no such experiments have been made at mK temperatures.

## References

- Aminov, L. K., and Teplov, M. A. (1990). *Sov. Sci. Rev. At. Phys.* **14**, 1.
- Argyle, B. E., Jantz, W., and Slonczewski, J. C. (1983). *J. Appl. Phys.* **54**, 3370.
- Baker, J. M., and Bleaney, B. (1958). *Proc. R. Soc. London* **245**, 156.
- Bleaney, B. (1988). In 'Handbook of Physics and Chemistry of Rare Earths' (Eds K. A. Gschneider and L. Eyring), pp. 397-8 (North Holland: Amsterdam).
- Cooke, A. H., Edmonds, D. T., Finn, C. B. F., and Wolf, W. P. (1968a). *Proc. R. Soc. London A* **306**, 313.
- Cooke, A. H., Edmonds, D. T., Finn, C. B. F., and Wolf, W. P. (1968b). *Proc. R. Soc. London A* **306**, 335.
- Dötsch, H. (1978). *IEE Trans. Mag.* **14**, 692.
- Dötsch, H., Röschmann, P., and Schilz, W. (1978). *Appl. Phys.* **15**, 167.
- Easley, W. C., Barclay, J. A., and Shirley, D. A. (1968). *Phys. Rev.* **170**, 1083.
- Fitzwater, D. R., and Rundle, R. E. (1959). *Z. Krystallogr.* **112**, 362.
- Fox, R. A., Hamilton, W. D., and Warner, D. D. (1974). *J. Phys. A* **7**, 1716.
- Hirvonen, M. T., Karla, T. E., Riski, K. J., Teplov, M. A., Malkin, B. Z., Phillips, N. E., and Wun, M. (1975). *Phys. Rev. B* **11**, 4652.
- Hufner, S. (1962). *Z. Phys.* **169**, 417.
- Ketelaar, J. A. A. (1937). *Physica (Utrecht)* **4**, 619.
- Krane, K. S., and Steffen, R. M. (1970). *Phys. Rev. C* **2**, 724.
- Krane, K. S., and Steffen, R. M. (1971). *Nucl. Phys. A* **164**, 439.
- Larsen, G. H., and Jeffries, C. D. (1966). *Phys. Rev.* **141**, 461.
- MacNeal, B. E., and Humphrey, F. B. (1979). *J. Appl. Phys.* **50**, 1010.
- Marshak, H., Brewer, W. D., Roman, P., Klein, E., Freitag, K., and Herzog, P. (1987). *Phys. Rev. Lett.* **59**, 1764.
- Neogy, D., Chatterji, A., and Neogy, A. (1978). *J. Chem. Phys.* **69**, 2703.
- Roman, P., Brewer, W. D., Klein, E., Marshak, H., Freitag, K., and Hertzog, P. (1986). *Phys. Rev. Lett.* **56**, 1976.
- Storey, B. E., Tooke, A. O., Cracknell, A. P., and Przystawa, J. A. (1977). *J. Phys. C* **10**, 875.
- Walker, L. R. (1957). *Phys. Rev.* **105**, 309.
- Walker, L. R. (1958). *J. Appl. Phys.* **29**, 318.